

Original research

Rupture risk prediction of cerebral aneurysms using a novel convolutional neural network-based deep learning model

Hyeondong Yang,¹ Kwang-Chun Cho ,² Jung-Jae Kim,³ Jae Ho Kim ,⁴ Yong Bae Kim,³ Je Hoon Oh¹

► Additional supplemental material is published online only. To view, please visit the journal online (<http://dx.doi.org/10.1136/neurintsurg-2021-018551>).

For numbered affiliations see end of article.

Correspondence to

Professor Je Hoon Oh, Mechanical Engineering and BK21 FOUR ERICA-ACE Center, Hanyang University, 55 Hanyangdaehak-ro, Sangnok-gu, Ansan, Gyeonggi-do 15588, Korea (the Republic of); jehoon@hanyang.ac.kr and Professor Yong Bae Kim, Department of Neurosurgery, College of Medicine, Yonsei University, Severance Hospital, 50-1 Yonsei-ro, Seodaemun-gu, Seoul 03722, Korea (the Republic of); ybkim69@yuhs.ac

HY and K-CC contributed equally.
YBK and JHO contributed equally.

HY and K-CC are joint first authors.

Received 12 December 2021
Accepted 24 January 2022
Published Online First
9 February 2022

ABSTRACT

Background Cerebral aneurysms should be treated before rupture because ruptured aneurysms result in serious disability. Therefore, accurate prediction of rupture risk is important and has been estimated using various hemodynamic factors.

Objective To suggest a new way to predict rupture risk in cerebral aneurysms using a novel deep learning model based on hemodynamic parameters for better decision-making about treatment.

Methods A novel convolutional neural network (CNN) model was used for rupture risk prediction retrospectively of 123 aneurysm cases. To include the effect of hemodynamic parameters into the CNN, the hemodynamic parameters were first calculated using computational fluid dynamics and fluid–structure interaction. Then, they were converted into images for training the CNN using a novel approach. In addition, new data augmentation methods were devised to obtain sufficient training data. A total of 53,136 images generated by data augmentation were used to train and test the CNN.

Results The CNNs trained with wall shear stress (WSS), strain, and combination images had area under the receiver operating characteristics curve values of 0.716, 0.741, and 0.883, respectively. Based on the cut-off values, the CNN trained with WSS (sensitivity: 0.5, specificity: 0.79) or strain (sensitivity: 0.74, specificity: 0.71) images alone was not highly predictive. However, the CNN trained with combination images of WSS and strain showed a sensitivity and specificity of 0.81 and 0.82, respectively.

Conclusion CNN-based deep learning algorithm using hemodynamic factors, including WSS and strain, could be an effective tool for predicting rupture risk in cerebral aneurysms with good predictive accuracy.

learning models trained with surface area and flatness to predict aneurysm stability.³ Heo *et al* trained machine learning models using health examination data that included age, sex, and blood pressure, and predicted the rupture risk of intracranial aneurysms.⁴ Furthermore, Kim *et al* constructed a deep learning model trained using three-dimensional digital subtraction angiography (3D-DSA) images of intracranial aneurysms and applied it to rupture prediction.⁵

Currently, hemodynamic parameters such as wall shear stress (WSS) are considered to be important factors for aneurysm formation and rupture risk.^{7,8} Many studies have applied computational fluid dynamics (CFD) to calculate hemodynamic parameters.^{9,10} Recently, fluid–structure interaction (FSI), which also considers the deformation of blood vessels, has been applied to overcome the limitations of CFD.^{11,12} In FSI analysis, strain is studied as an important hemodynamic factor for aneurysm rupture risk.¹¹ However, the strain has yet to be considered in predicting the rupture risk of cerebral aneurysms using deep learning.

In this study, to more accurately predict rupture risk of cerebral aneurysms, we suggested a novel deep learning model based on a convolutional neural network (CNN) which can fully consider the effects of WSS and strain. To this end, the hemodynamic parameters were first calculated using CFD and FSI, and then converted into images for training the CNN using a novel approach. Subsequently, the CNN-based deep learning model was trained with images of WSS and strain to predict rupture risk. Finally, the performance of the novel deep learning model was evaluated using test dataset that were not used for training.

METHODS

The study protocol was approved by our institutional review board, and the need for written informed consent was waived. A total of 123 patients with cerebral aneurysms were recruited between April 2014 and January 2021. All data were prospectively recorded in the databases and reviewed retrospectively. The inclusion criteria were as follows: (1) adult patients over 18 years old, (2) a diagnosis of saccular aneurysms located in the anterior circulation, and (3) patients with DSA source data available for computer simulation. The exclusion criteria were as follows: (1) a diagnosis of

INTRODUCTION

Spontaneous subarachnoid hemorrhage caused by a ruptured cerebral aneurysm results in serious disability.^{1,2} Therefore, early diagnosis and operation before rupture are important to improve clinical outcomes.

Recently, owing to the development of artificial intelligence, technologies such as machine learning and deep learning have been applied to medical fields.^{3–6} Artificial intelligence has been used to aid the detection of cerebral aneurysms and also to predict ruptures.^{5,6} Liu *et al* developed machine



© Author(s) (or their employer(s)) 2023. No commercial re-use. See rights and permissions. Published by BMJ.

To cite: Yang H, Cho K-C, Kim J-J, *et al*. *J NeuroInterv Surg* 2023;**15**:200–204.

non-saccular aneurysms, (2) aneurysms located in the posterior circulation, and (3) patients with a previous history of surgical clipping or coil embolization.

Of the 123 aneurysm cases, 75 (53 unruptured aneurysms and 22 ruptured aneurysms) were extracted randomly for the training dataset, while the remaining 48 (26 unruptured aneurysms and 22 ruptured aneurysms) were classified into the test dataset.

Unlike the cases of unruptured aneurysms, in the cases of several ruptured aneurysms, we found that blood which spilled out of the aneurysm formed a pseudo-sac. Therefore, following the elimination method used in the previous study,¹³ the pseudo-sac was removed to delineate the assumed original model before rupture (online supplemental figure S1). Of a total of 44 ruptured cases, 8 were modified.

CFD and FSI analyses

The hemodynamic parameters, WSS and strain, were extracted at the thin wall area (TWA) for more effective analysis. Cho *et al* conducted the study predicting the location of the TWA using CFD.¹⁴ As a result of analyzing the location of the TWA in the intraoperative images, they confirmed that the location of the low WSS was highly related to the location of the TWA. Therefore, it was assumed that the location where the low WSS occurs is the location of TWA.

CFD was conducted to predict the location of the TWA and calculate the WSS in the TWA. The blood was considered to be an incompressible Newtonian fluid with a density of 1,055 kg/m³ and a viscosity of 0.004 kg/m·s. Additionally, the pulsatile flow with a Womersley velocity profile and the pressure profile to adjust the pressure of the carotid artery were applied to the inlet and outlet conditions, respectively.^{14 15} The blood vessel model was assumed to be a rigid wall with a non-slip condition. CFD analysis was performed using ANSYS Workbench Fluent (version 19.2, ANSYS Inc., Canonsburg, Philadelphia, USA).

FSI was used to calculate the strain considering the deformation of the blood vessel. Young's modulus of the blood vessel was assumed to be 1.5 MPa, and the wall thickness of the blood vessel was assumed to be 0.36 mm.¹⁶ To specify that the TWAs have lower Young's modulus and thinner walls than other regions, Young's modulus and the wall thickness of the TWA were set as 0.375 MPa and 0.09 mm, respectively, which is 25 % of the normal values of the Young's modulus and thickness.¹¹ All df of the inlet and outlet were constrained as fixed, and Poisson's ratio was set to 0.49. In both the CFD and FSI analyses, one cardiac cycle was divided into 64 steps. In this study, the word 'strain' refers to the equivalent strain, which expresses the strain components of each direction as a single value.

Generation of training data and test data from CFD and FSI analyses

To construct the CNN-based deep learning models, the WSS calculated from CFD, and strain calculated from FSI, were converted to grayscale images (figure 1A). First, the location of the TWA was predicted using CFD. The point with the smallest WSS value in the TWA was assumed to be the center of the TWA, and a small circle around the center point was constructed. Subsequently, four points were determined in a clockwise direction at 90° intervals starting from an arbitrary point on the circle. Second, the values of WSS and strain were extracted at the positions of the five previously determined points during one cardiac cycle, and they were normalized to have a value between 0 and 1 to minimize the influence of analysis conditions.¹⁴ Then, using

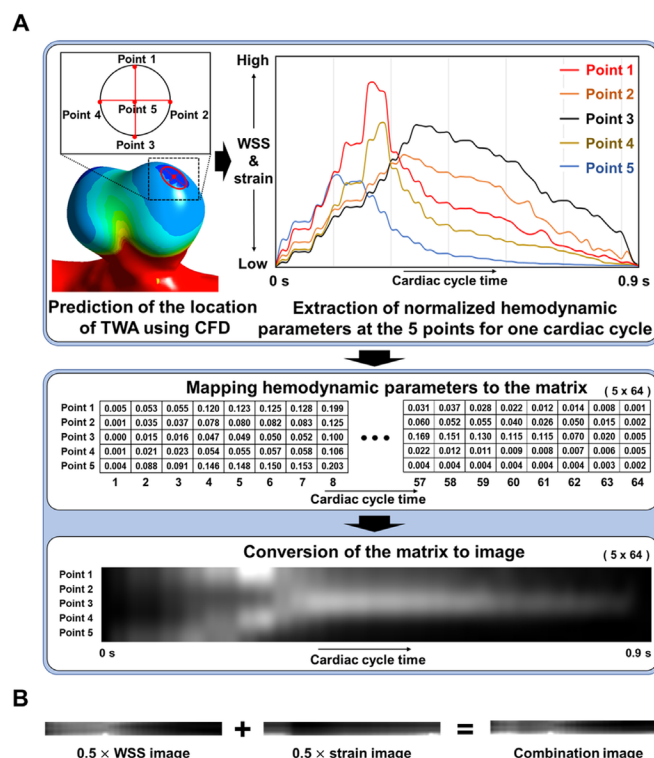


Figure 1 (A) Process of creating images for deep learning from simulations. (B) Method of generating a combination image using a wall shear stress and strain image. CFD, computational fluid dynamics; TWA, thin-wall area; WSS, wall shear stress.

the 64 data points calculated in one cardiac cycle from each of the five points, a 5 × 64 matrix was created. Finally, the matrix was converted to a grayscale image.

In addition, to consider the characteristics of various hemodynamic parameters, the images generated using the WSS values (WSS image) and the images generated using the strain values (strain image) were merged. New combination images were created by combining WSS and strain images with equal weights (figure 1B).

Data augmentation

Because CNN-based deep learning models require large training datasets, we devised new data augmentation methods making the most of computer simulations (figure 2). Three types of data augmentation methods were used in this study. First, by increasing the radius of the circle constructed at the center point of the TWA, new points were added for generating the images. The radius of the circle was set to 0.5, 0.75, and 1 mm. Second, the new points were augmented by rotating the circle from 0° to 90° at intervals of 5°. Third, data augmentation was performed by changing the order in which the points were listed. New images were created by changing the order in which the points were listed from points 1 to 4 and by changing the rotation direction from clockwise to counterclockwise. A total of 432 images were created from one simulation case using these data augmentation methods, and a total of 53,136 images were obtained from the 123 cases considered in this study.

Construction of deep learning models

CNNs are considered a leading tool for medical image analysis.⁵ The main advantage of CNNs is that they can find complex features such as higher-order statistics and non-linear correlations

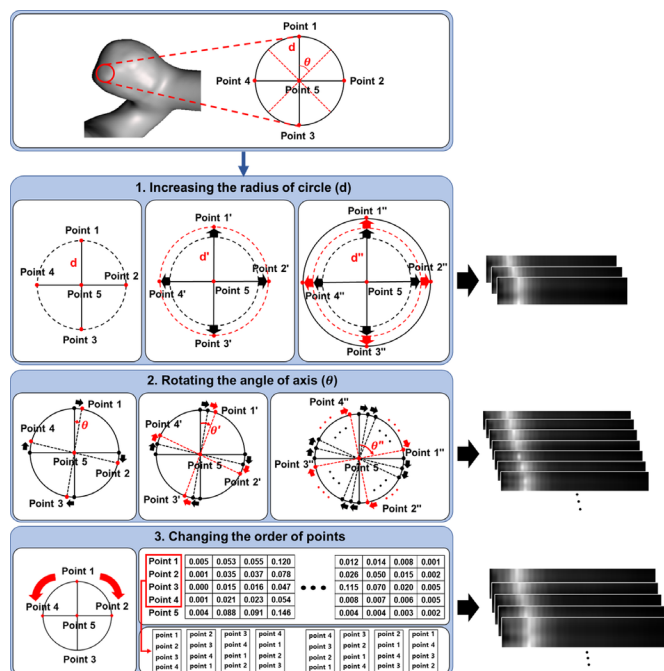


Figure 2 Data augmentation methods: increasing the radius of the circle, rotating the axis, and changing the order of the points.

in images,¹⁷ which are difficult for humans to distinguish. Therefore, in this study, the CNN was used to construct the deep learning models. Figure 3 shows the entire process and CNN architecture for the rupture prediction by training the images generated from CFD and FSI. In addition, the detailed calculation process of the CNN is illustrated in online supplemental figure S2. The CNN models were constructed using Tensorflow.

When an image is inputted into the deep learning model, its rupture risk is evaluated by calculating a constant value between 0 and 1 through the internal process in the model. The deep learning model calculates a value closer to 1 when the input data is determined to be closer to a ruptured case. Conversely, as the model determines that the input data is closer to an unruptured case, a value closer to 0 is computed. Therefore, the deep learning model expresses the probability of whether the input data would indicate a rupture based on the computed value between 0 and 1, which we referred to as the rupture risk.

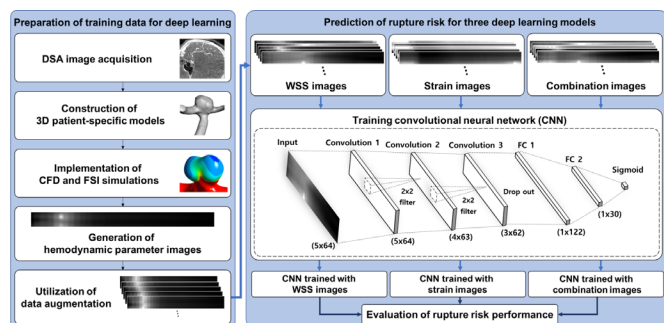


Figure 3 CNN-based deep learning process and CNN architecture. CFD, computational fluid dynamics; CNN, convolutional neural network; DSA, digital subtraction angiography; FSI, fluid–structure interaction; WSS, wall shear stress.

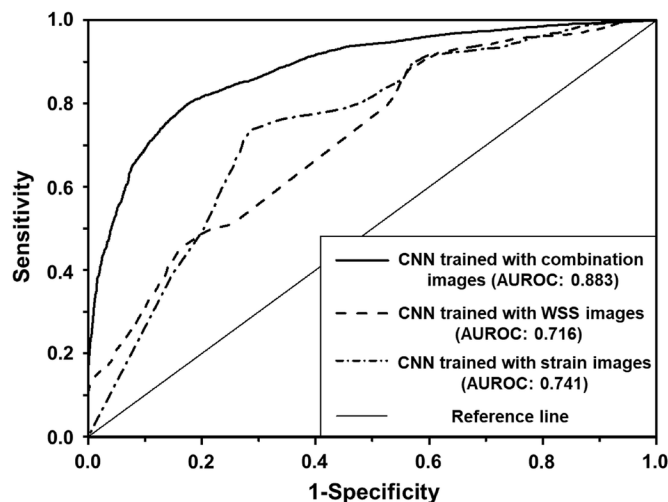


Figure 4 Receiver operating characteristic curves of the CNN trained with combination, WSS only and strain only images for test set. AUROC, area under the receiver operating characteristics; CNN, convolutional neural network; WSS, wall shear stress.

Statistical analyses

The area under the receiver operating characteristic (AUROC) curve was calculated to evaluate the performance of the CNN-based deep learning model. The cut-off value was determined using Youden's index based on the receiver operating characteristic (ROC) curve. All statistical analyses were performed using IBM SPSS Statistics version 24.0 (IBM Corp., Armonk, New York, USA).

RESULTS

Datasets

The training set comprises 75 aneurysms, ranging from 2.6 to 11.2 mm in the maximum diameter (mean size 5.5 mm), from 72 patients (48 women and 24 men). The mean age of the patients in the training set was 57.6 years (range, 27–84 years). For the test set of 48 aneurysms from 48 patients (37 women and 11 men), the aneurysm sizes ranged from 2.9 to 12.0 mm in the maximum diameter (mean size, 6.4 mm). The mean age of the patients in the test set was 58.5 years (range 28–84 years). Online supplemental figure S3 shows examples of the WSS, strain, and combination images created from CFD and FSI analyses for unruptured (online supplemental figure S3A) and ruptured cases (online supplemental figure S3B).

Mean and SD of parameters for unruptured and ruptured aneurysms in test set are listed in online supplemental table S1. (Comparisons of unruptured and ruptured aneurysms for several morphological parameters in the test set are also shown in online supplemental table S1.) For the test set, there was no significant statistical difference in morphological parameters between the unruptured and ruptured aneurysms.

Diagnostic performance

Figure 4 shows the ROC curves of the CNNs trained with WSS, strain, and combination images. When performances of the CNN models were evaluated using the test set, the AUROC value of the CNN trained with the combination images was the highest. The CNNs trained with WSS, strain, and combination images had AUROC values of 0.716, 0.741, and 0.883, respectively. Based on the cut-off value determined using Youden's index, the CNN trained with combination images also produced the highest the

sensitivity and specificity. The sensitivity and specificity of the CNN trained with only WSS images were 0.5 and 0.79, respectively, and those of the CNN trained with only strain images were 0.74 and 0.71, respectively. The corresponding values of the CNN trained with combination images were 0.81 and 0.82, respectively.

DISCUSSION

Application of FSI analysis

Several morphologic factors, including the size ratio and aspect ratio, have been used for predicting the rupture risk of cerebral aneurysms.¹⁸ More recently, various hemodynamic parameters have been studied to identify their relations with aneurysmal rupture risk.^{19,20} A recent systematic review and meta-analysis by Can and Du found that a high WSS was associated with intracranial aneurysm formation, and a low WSS was related to intracranial aneurysm rupture.⁷ However, despite their findings, there is still controversy about the exact role of WSS in the growth and rupture of aneurysms.²¹ One of the possible reasons for this inconsistency is the intrinsic limitation of the CFD analysis.^{21,22} This is a natural limitation in that the effects of wall thickness and mechanical properties of the blood vessels are ignored in the CFD analysis.¹¹ To overcome this critical limitation, we used the FSI analysis, which assumes that the blood vessel is deformable rather than rigid; thus, the mechanical properties of the aneurysms and effects of the wall thickness can be evaluated in a more realistic manner.¹¹ Therefore, we constructed the CNN-based deep learning model using WSS from CFD analysis and strain from FSI analysis.

Novel method of data augmentation

A large amount of data is crucial for successful application of CNNs. To date, numerous studies have used computer simulations, such as CFD and FSI, to analyze the characteristics of hemodynamic parameters of cerebral aneurysms. However, the critical limitation of these computer simulations is that it is infeasible to collect sufficiently large amounts of data for CNNs.

In the field of medical imaging, as the deep learning technique advances, data augmentation methods have been studied to generate large datasets from small datasets.^{23,24} However, the data augmentation method that has been used so far simply creates multiple identical images by rotating or translating a single image. If the images created through this augmentation method have the same information, the training through the deep learning model is not efficient and satisfactory.

Instead of using real medical images such as DSA and CT images, we devised a whole new approach to create artificial images of hemodynamic parameters calculated from simulation and developed a novel data augmentation method. Since the augmented images from the new method have different information, it is more effective for the deep learning model to learn various types of information. This novel data augmentation method could make it possible to overcome the limitations of computer simulations for cerebral aneurysms. Furthermore, it would be expected that CNN with both computer simulation and data augmentation paves the way for applying hemodynamic parameters to actual clinical practices.

Diagnostic accuracy with combination images

CNNs have been widely used in studies on cerebrovascular diseases using deep learning. Kim *et al* reported an overall diagnostic accuracy of 76.84% in aneurysm rupture predictions (sensitivity 78.76 %, specificity 72.15 %).⁵ In their study, the

AUROC in the CNN was 0.755, which was better than that obtained by a human evaluator.⁵

In our study, the CNN trained with combination images of WSS and strain had a sensitivity of 0.81 and a specificity of 0.82 for predicting aneurysm rupture risk and showed an AUROC of 0.883 with test set cases. Although there was no significant difference in morphological parameters between ruptured and unruptured groups in the test set, the meaningful difference between the two groups was observed when hemodynamic parameters calculated using our method were included in the test set. Furthermore, these results show better performance than those of previous studies.^{3,5}

The CNN trained with combination images performed better than the CNNs trained with WSS or strain images alone. WSS is a parameter that represents the blood flow characteristics inside a blood vessel and is known to have a dominant effect on aneurysm rupture due to its relationship with endothelial cells.²⁵ Mechanical stretch of vascular wall is another major parameter for understanding the aneurysm rupture mechanism. Mechanical stretching of the extracellular matrix of the vascular wall leads to reconstitution and degeneration.²⁶ The strain is calculated as the ratio of the deformation to the initial length and indicates the degree of blood vessel deformation. Therefore, the strain is the most appropriate parameter for mechanical stretching.

Thus, by simultaneously considering the two parameters of WSS and strain, the blood flow characteristics and also the structural characteristics of the blood vessels can be reflected in the deep learning model. For this reason, it appears that the performance of the CNN trained with the combination images of WSS and strain was better than that of the CNNs trained with one parameter alone.

Future clinical applications

In this study, we suggested a novel CNN-based deep learning model and investigated the effects of hemodynamic factors on the prediction of patient-specific risk of aneurysmal rupture. Previously, aneurysm rupture risk has been predicted using the clinical characteristics of the patients and morphological factors of aneurysms. However, aneurysm rupture risk will be predicted by taking into account the effects of individual patient-specific hemodynamic factors. With the help of the proposed CNN-based deep learning model, the rupture risk of cerebral aneurysms could be evaluated using hemodynamic factors. In clinical practice, the rupture risk of an aneurysm could be evaluated by referencing this value obtained from our prediction model with the cut-off value from Youden's index of the ROC curve. The use of computer simulation has several constraints, including the required time and background knowledge. To overcome these challenges, the deep learning technique as a tool for replacing the simulation process has been investigated.^{27,28} If these studies are conducted continuously, clinicians can obtain information on the rupture risk within a relatively short time, which may help to facilitate clinical application and enable more accurate decisions.

Limitations

We obtained the three-dimensional geometric data of aneurysms from DSA. However, 3D-DSA data for the ruptured aneurysms were obtained after rupture of the aneurysmal sac; thus, eight out of 44 ruptured aneurysms cases had a pseudo-sac due to blood spill from the aneurysms. To deal with this problem, we carefully removed the pseudo-sac and restored the original shape before rupture; however, this might not accurately reflect the aneurysmal morphology before rupture.

Another limitation is that the data used in this study were not completely patient-specific. The thickness and material properties of blood vessels differ depending on the patient, as do the pressure and the flow rate in the blood vessels. In the past, it was difficult to obtain the flow rate for each patient, although it has become relatively easier owing to the development of four-dimensional magnetic resonance imaging (4D-MRI) these days. Our future work will use this 4D-MRI to obtain patient-specific flow data and apply them to the hemodynamic analysis. More realistic results are likely to be obtained if these limitations are overcome.

Strictly speaking, this study has shown the results of cross-sectional judgment, not the longitudinal follow-up of an unruptured cerebral aneurysm. Because there were still insufficient data to perform a reliable longitudinal study, we conducted a cross-sectional study. However, considering that unruptured aneurysms remained stable during the period of this study, we believe that the suggested prediction method could be used as a surrogate marker to supplement the existing predictors.

Because computer simulations still have several limitations, there was a limit to improving the performance of the rupture risk for our deep learning model. It is our future work to generate a more accurate rupture risk prediction method by considering commonly used morphological parameters such as aspect ratio and size ratio together with hemodynamic parameters in the deep learning model.

CONCLUSIONS

In the present study, we propose a novel CNN-based deep learning model using important hemodynamic factors, such as WSS and strain, to predict the rupture risk of cerebral aneurysms. The results showed high sensitivity and high specificity, and this novel method could be used to predict the rupture risk of cerebral aneurysms.

Author affiliations

¹Department of Mechanical Engineering and BK21 FOUR ERICA-ACE Center, Hanyang University, Ansan, Gyeonggi-do, Korea

²Department of Neurosurgery, College of Medicine, Yonsei University, Yonjin Severance Hospital, Yonjin, Korea

³Department of Neurosurgery, College of Medicine, Yonsei University, Severance Hospital, Seoul, Korea

⁴Department of Neurosurgery, College of Medicine, Chosun University, Chosun University Hospital, Gwangju, Korea

Contributors HY and K-CC contributed equally to this work as co-first authors. JHO and YBK contributed equally to this work as co-corresponding authors. HY and K-CC gathered the data and drafted the manuscript in collaboration. J-JK and JHK assisted in the discussions and reviewed the manuscript. JHO and YBK conceptualized the study and supervised the process, corresponding to each field of specialty. All authors approved the final version of the manuscript. JHO and YBK are guarantors of this work.

Funding This work was supported by the National Research Foundation of Korea (NRF) grant funded by the Korea government (No. 2020R1A2C1011918). It was also supported by the NRF grant funded by the Korea government (No. 2021R1F1A1049435).

Competing interests None declared.

Patient consent for publication Not applicable.

Ethics approval This study involves human participants and was approved by Yonsei University Gangnam Severance Hospital, institutional review board3-2019-0178.

Provenance and peer review Not commissioned; externally peer reviewed.

Data availability statement No data are available.

Supplemental material This content has been supplied by the author(s). It has not been vetted by BMJ Publishing Group Limited (BMJ) and may not have been peer-reviewed. Any opinions or recommendations discussed are solely those of the author(s) and are not endorsed by BMJ. BMJ disclaims all liability and

responsibility arising from any reliance placed on the content. Where the content includes any translated material, BMJ does not warrant the accuracy and reliability of the translations (including but not limited to local regulations, clinical guidelines, terminology, drug names and drug dosages), and is not responsible for any error and/or omissions arising from translation and adaptation or otherwise.

ORCID iDs

Kwang-Chun Cho <http://orcid.org/0000-0002-0261-9283>

Jae Ho Kim <http://orcid.org/0000-0002-6292-5223>

REFERENCES

- 1 Broderick JP, Brott TG, Duldner JE, *et al.* Initial and recurrent bleeding are the major causes of death following subarachnoid hemorrhage. *Stroke* 1994;25:1342–7.
- 2 White PM, Wardlaw JM. Unruptured intracranial aneurysms. *J Neuroradiol* 2003;30:336–50.
- 3 Liu Q, Jiang P, Jiang Y, *et al.* Prediction of aneurysm stability using a machine learning model based on PyRadiomics-derived morphological features. *Stroke* 2019;50:2314–21.
- 4 Heo J, Park SJ, Kang S-H, *et al.* Prediction of intracranial aneurysm risk using machine learning. *Sci Rep* 2020;10:6921.
- 5 Kim HC, Rhim JK, Ahn JH, *et al.* Machine learning application for rupture risk assessment in small-sized intracranial aneurysm. *J Clin Med* 2019;8:683.
- 6 Shi Z, Hu B, Schoepf UJ, *et al.* Artificial intelligence in the management of intracranial aneurysms: current status and future perspectives. *AJNR Am J Neuroradiol* 2020;41:373–9.
- 7 Can A, Du R. Association of hemodynamic factors with intracranial aneurysm formation and rupture: systematic review and meta-analysis. *Neurosurgery* 2016;78:510–20.
- 8 Suzuki T, Stapleton CJ, Koch MJ, *et al.* Decreased wall shear stress at high-pressure areas predicts the rupture point in ruptured intracranial aneurysms. *J Neurosurg* 2019;132:1–7.
- 9 Murayama Y, Fujimura S, Suzuki T, *et al.* Computational fluid dynamics as a risk assessment tool for aneurysm rupture. *Neurosurg Focus* 2019;47:E12.
- 10 Hua Y, Oh JH, Kim YB. Influence of parent artery segmentation and boundary conditions on hemodynamic characteristics of intracranial aneurysms. *Yonsei Med J* 2015;56:1328–37.
- 11 Cho K-C, Yang H, Kim J-J, *et al.* Prediction of rupture risk in cerebral aneurysms by comparing clinical cases with fluid-structure interaction analyses. *Sci Rep* 2020;10:18237.
- 12 Kim J-J, Yang H, Kim YB, *et al.* The quantitative comparison between high wall shear stress and high strain in the formation of paraclinoid aneurysms. *Sci Rep* 2021;11:7947.
- 13 Russell JH, Kelson N, Barry M, *et al.* Computational fluid dynamic analysis of intracranial aneurysmal bleb formation. *Neurosurgery* 2013;73:1061–9. discussion 8–9.
- 14 Cho K-C, Choi JH, Oh JH, *et al.* Prediction of thin-walled areas of unruptured cerebral aneurysms through comparison of normalized hemodynamic parameters and intraoperative images. *Biomed Res Int* 2018;2018:1–9.
- 15 Raymond P, Merenda F, Perren F, *et al.* Validation of a one-dimensional model of the systemic arterial tree. *Am J Physiol Heart Circ Physiol* 2009;297:H208–22.
- 16 Alastruey J, Parker KH, Peiró J, *et al.* Modelling the circle of Willis to assess the effects of anatomical variations and occlusions on cerebral flows. *J Biomech* 2007;40:1794–805.
- 17 Cuadrado-Godia E, Dwivedi P, Sharma S, *et al.* Cerebral small vessel disease: a review focusing on pathophysiology, biomarkers, and machine learning strategies. *J Stroke* 2018;20:302–20.
- 18 Kleinloog R, de Mul N, Verweij BH, *et al.* Risk factors for intracranial aneurysm rupture: a systematic review. *Neurosurgery* 2018;82:431–40.
- 19 Cornelissen BMW, Schneiders JJ, Potters WV, *et al.* Hemodynamic differences in intracranial aneurysms before and after rupture. *AJNR Am J Neuroradiol* 2015;36:1927–33.
- 20 Lv N, Karmonik C, Chen S, *et al.* Wall enhancement, hemodynamics, and morphology in unruptured intracranial aneurysms with high rupture risk. *Transl Stroke Res* 2020;11:882–9.
- 21 Cebal JR, Meng H. Counterpoint: realizing the clinical utility of computational fluid dynamics—closing the gap. *AJNR Am J Neuroradiol* 2012;33:396–8.
- 22 Robertson AM, Watton PN. Computational fluid dynamics in aneurysm research: critical reflections, future directions. *AJNR Am J Neuroradiol* 2012;33:992–5.
- 23 Nalepa J, Marcinkiewicz M, Kawulok M. Data augmentation for brain-tumor segmentation: a review. *Front Comput Neurosci* 2019;13:83.
- 24 Islam KT, Wijewickrema S, O'Leary S. A rotation and translation invariant method for 3D organ image classification using deep convolutional neural networks. *PeerJ Comput Sci* 2019;5:e181.

- 25 Etminan N, Rinkel GJ. Unruptured intracranial aneurysms: development, rupture and preventive management. *Nat Rev Neurol* 2016;12:699–713.
- 26 Liu P, Song Y, Zhou Y, *et al.* Cyclic mechanical stretch induced smooth muscle cell changes in cerebral aneurysm progress by reducing collagen type IV and collagen type VI levels. *Cell Physiol Biochem* 2018;45:1051–60.
- 27 Liang L, Mao W, Sun W. A feasibility study of deep learning for predicting hemodynamics of human thoracic aorta. *J Biomech* 2020;99:109544.
- 28 Madani A, Bakhaty A, Kim J, *et al.* Bridging finite element and machine learning modeling: stress prediction of arterial walls in atherosclerosis. *J Biomech Eng* 2019. doi:10.1115/1.4043290. [Epub ahead of print: 26 Mar 2019].